Xu-Sheng Liu*, Shao-Yi Wu, Meng Han* and Qing-Sheng Zhu

Theoretical Studies of the Defect Structures for $Cu(en)_3^{2+}$ and $Ru(en)_3^{3+}$ Clusters in Tris(Ethylenediamine) Complexes

https://doi.org/10.1515/zna-2019-0358 Received December 5, 2019; accepted January 12, 2020; previously published online February 7, 2020

Abstract: The local structures and spin Hamiltonian parameters (SHPs, g factors, and hyperfine structure constants) for the Cu(en)₃²⁺ and Ru(en)₃³⁺ clusters in ethylenediamine complexes are theoretically studied from perturbation formulae for tetragonally and trigonally elongated octahedral 3d⁹ and 4d⁵ clusters, respectively. Cu²⁺ centres I and II may experience the slight relative elongations ΔZ by about 0.005 and 0.007 Å in Zn(en)₃(NO₃)₂ polycrystalline powder at 4.2 K and room temperature, respectively, along the C₄ axis arising from the Jahn-Teller effect. For Ru(en)₃³⁺ cluster in the uniaxial [Rh(en)₃Cl₃]₂NaCl · 6H₂O single crystal doped with the single-crystal chloride salt [Ru(en)₃]Cl₃·4H₂O, the local impurity-ligand bonding angle related to the C3 axis suffers a negative variation $\Delta\beta$ (\approx -1.85°) with respect to the host β_H in $[Ru(en)_3]Cl_3 \cdot 4H_2O$ at 4 K. The features of SHPs and defect structures for the $Cu(en)_3^{2+}$ and $Ru(en)_3^{3+}$ clusters are also discussed in view of the different experimental temperatures.

Keywords: $Cu(en)_3^{2+}$; Defect Structures; Electron Paramagnetic Resonance; Ethylenediamine Complexes; $Ru(en)_3^{3+}$.

1 Introduction

Ethylenediamine (en) and the relevant complexes have broad applications in a diverse range of fields. Ethylenediamine can improve enzymatic digestibility of corn stover

*Corresponding authors: Xu-Sheng Liu, Department of
Applied Physics, School of Physics, University of Electronic
Science and Technology of China, Chengdu 610054, China,
E-mail: xsliu999@126.com; and Meng Han, School of Public Affairs
and Administration, University of Electronic Science and Technology
of China, Chengdu 611731, China, E-mail: hmuestc@126.com
Shao-Yi Wu and Qing-Sheng Zhu: Department of Applied Physics,
School of Physics, University of Electronic Science and Technology
of China, Chengdu 610054, China

for the production of fermentable sugars [1] and act as a vapour phase crosslinking agent for Matrimid films in the range of 0.35-0.55 µm under ambient conditions for alcohol penetrant transport [2]. In particular, the various ethylenediamine complexes can be used as fluorescent sensors [3] and fluorescence probes for detecting Hg²⁺ in water [4], as well as fluffy porous carbon nanotube composites for isolation of clenbuterol from pork [5]. On the other hand, ruthenium (e.g. Ru³⁺) and ruthenium complexes not only can act as an electrogenerated chemiluminescence label for highly sensitive detection of DNA methylation and assay of methyltransferases activity [6], but also exhibit giant magnetoresistance [7]. Moreover, the tris(ethylenediamine)ruthenium (III) (4d⁵) complex, $Ru(en)_3^{3+}$, can be adopted as a water oxidation catalyst for the cooperative catalysis of the bimolecular decomposition with high concentrations in aqueous solution [8] and the chemically modified electrodes in chemical sensors [9]. Copper (Cu²⁺, 3d⁹) is a vital transition-metal element in cofactor for protein enzymes [10], antimicrobial activity against the bacteria Salmonella paratyphi [11], modification of DNA [12], and high T_C superconductivity [13]. Furthermore, both Cu²⁺ and Ru³⁺ under octahedra exhibit orbitally degenerated ground states and thus experience the Jahn-Teller distortions through the vibration interaction [14-16]. These systems may demonstrate unique structural properties that are of special scientific significance.

As the single crystals of transition-metal complexes in the form of $M(en)_3^{n+}$ are ideal host lattices for the studies of the local structures and electronic properties, considerable researches have been conducted by means of electron paramagnetic resonance (EPR) [17, 18], reversible phase transitions [19], and the circularly polarised luminescence spectra [20] and vibrational dichroism spectroscopy [21]. Especially, EPR is a very informative method to probe the delicate local distortions of the active transition-metal centres, characterised by the spin Hamiltonian parameters (SHPs), i.e. g factors and hyperfine structure constants. Electron paramagnetic resonance spectra were measured for the trigonally distorted Ru(en) $_3^{3+}$ in the uniaxial $[Rh(en)_3Cl_3]_2NaCl\cdot 6H_2O$ single crystal doped with

the single-crystal chloride salt [Ru(en)₃]Cl₃·4H₂O at 4 K and the two tetragonally elongated octahedral Cu(en)₃²⁺ clusters in Zn(en)₃(NO₃)₂:Cu²⁺ polycrystalline powder at 4.2 K and room temperature (RT), respectively [17, 18]. Regretfully, these experimental results of EPR spectra have not been theoretically analysed until now; neither has the quantitative formation about the local structures of these clusters been obtained. In view of the importance of the mechanisms of the SHPs and the local structural information for the above $Cu(en)_3^{2+}$ and $Ru(en)_3^{3+}$ clusters, which have been rather scarcely studied so far, it is worthy to perform further investigations on their SHPs and local structures in a uniform way so as to achieve deep understanding of the structures and properties for ethylenediamine complexes containing transition-metal impurities. In this work, the SHPs and local structures of these transitionmetal clusters are theoretically and systematically investigated based on the perturbation formulae of the SHPs for trigonally distorted octahedral 4d⁵ and tetragonally elongated octahedral 3d9 clusters. The reasonableness of the results and the local structures of the various Ru(en)₃³⁺ and $Cu(en)_3^{2+}$ clusters are discussed.

2 Theoretical Calculations

2.1 Local Structures of the $Cu(en)_3^{2+}$ and $Ru(en)_3^{3+}$ Clusters

For the $Cu(en)_3^{2+}$ clusters in the $Zn(en)_3(NO_3)_2$ polycrystalline powder, the octahedral Cu²⁺ is coordinated to six nitrogen atoms (from three en groups) and forms two tetragonally elongated octahedral centres at 4.2 K (centre I) and RT (centre II) [18], respectively. As $Cu^{2+}(3d^9)$ is a Jahn-Teller ion, the Cu(en)₃²⁺ clusters may undergo the significant Jahn-Teller effect through the vibration interactions and generate six magnetically nonequivalent sites. As a result, both copper centres exhibit the tetragonal elongation distortions, responsible for the feature of the observed g factors $(g_{\parallel} > g_{\perp} \ge 2$ [18]). The energy level structure for a $Cu^{2+}(3d^9)$ ion under ideal octahedra can be described as a ground orbital doublet ${}^{2}E_{g}$ and an excited orbital triplet ${}^2T_{2g}$ [22, 23]. Subject to the tetragonal elongation distortion, the two-fold orbital degeneracy of the cubic ${}^{2}E_{g}$ ground state can be lifted by the Jahn-Teller effect and separated into two orbital singlets ${}^{2}B_{1g}$ and ${}^{2}A_{1g}$, with the former lying lowest [24, 25]. Therefore, the local impurity-ligand bond lengths (R_{\parallel} and R_{\perp}) parallel and perpendicular to the C4 axis may be conveniently characterised by a relative tetragonal elongation ΔZ (Fig. 1a).

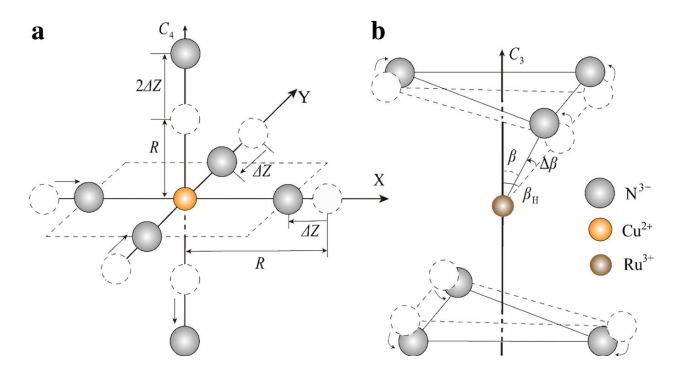


Figure 1: Local structures of the tetragonally elongated octahedral $Cu(en)_3^{2+}$ (a) and the trigonally distorted octahedral $Ru(en)_3^{3+}$ (b) clusters characterised by the relative tetragonal elongation ΔZ and the angular variation $\Delta \beta$, respectively.

The Ru(en)₃³⁺ cluster is formed in the diamagnetic and uniaxial solvent [Rh(en)₃Cl₃]₂NaCl·6H₂O doped with the single-crystal chloride salt $[Ru(en)_3]Cl_3 \cdot 4H_2O$, which may tend to conserve the original trigonal (D_{3d}) symmetry [17]. As Ru³⁺ (4d⁵) is also a Jahn–Teller ion with the ground orbital triplet ${}^2T_{2g}$ in an ideal octahedron, the Ru(en)₃³⁺ cluster can undergo the Jahn–Teller distortion through the vibration interaction and bring forward some modification in the local structure [26-29]. In addition, slightly different environments for the Ru(en)₃³⁺ cluster in the solvent of [Rh(en)₃Cl₃]₂NaCl·6H₂O single crystal may also lead to some influence on the local structure related to that in the solute $[Ru(en)_3]Cl_3 \cdot 4H_2O$. Under trigonally elongated octahedra, the cubic ground ${}^2T_{2g}$ state of low spin (S = 1/2) may split into one orbital singlet ${}^2A_{1g}$ and one doublet ${}^{2}E_{g}$, with the later lying lowest [22, 30]. The above energy separation is often defined as the trigonal field parameter V [22, 30, 31]. Moreover, the spinorbit coupling interactions may induce the further splittings of these states into three Kramers doublets. In view of the host metal–ligand bonding angle β_H (≈57.32° [17, 32]) of Ru³⁺ site in the solute [Ru(en)₃]Cl₃·4H₂O, the structural modifications of this trigonal centre can be suitably described as the angular variation $\Delta\beta$ (= $\beta - \beta_H$) of the local Ru^{3+} – N^{3-} bonding angle β in the solvent related to the host bonding angle β_H in the solute (Fig. 1b).

2.2 Calculations for Two Cu²⁺ Centres in Zn(en)₃(NO₃)₂ Single Crystal

For a $3d^9$ ion in tetragonally elongated octahedra, the lower cubic orbital doublet ${}^2E_{\rm g}$ would be separated into two orbital singlets ${}^2B_{\rm 1g}$ ($|{\rm x}^2-{\rm y}^2>$) and ${}^2A_{\rm 1g}(|{\rm z}^2>)$, and the former is the lowest [22, 23]. The higher cubic orbital triplet ${}^2T_{\rm 2g}$ may split into an orbital singlet ${}^2B_{\rm 2g}$ ($|{\rm xy}>$) and a doublet ${}^2E_{\rm g}(|{\rm xz}>,|{\rm yz}>)$ [22, 23]. In order to study the EPR

spectra and the local structures for the two Cu²⁺ centres in Zn(en)₃(NO₃)₂ single crystal at 4.2 K and RT, the fourthorder perturbation formulae [33] of SHPs for a tetragonally elongated octahedral 3d⁹ cluster may be adopted here. As the studied Cu²⁺ centres in the ethylenediamine composite have significant covalence and ligand orbital and spinorbit coupling interactions, the perturbation formulae of the SHPs based on the cluster approach [34-37] including the ligand contributions are involved here. Thus, we have

$$g_{\parallel} = g_{s} + 8k'\zeta'/W_{1} + k\zeta'^{2}/W_{2}^{2} + 4k'\zeta\zeta'/(W_{1}W_{2})$$

$$+ g_{s}\zeta'^{2}[1/W_{1}^{2} - 1/(2 W_{2}^{2})]$$

$$- k\zeta\zeta'^{2}(4/W_{1} - 1/W_{2})/W_{2}^{2}$$

$$- 2k'\zeta\zeta'^{2}[2/(W_{1}W_{2}) - 1/W_{2}^{2}]/W_{1}$$

$$- g_{s}\zeta\zeta'^{2}\Big[1/\Big(W_{1}W_{2}^{2}\Big) - 1/\Big(2 W_{2}^{3}\Big)\Big],$$

$$g_{\perp} = g_{s} + 2k'\zeta'/W_{2} - 4k\zeta'^{2}/(W_{1}W_{2})$$

$$+ k'\zeta\zeta'(2/W_{1} - 1/W_{2})/W_{2} + 2g_{s}\zeta'^{2}/W_{1}^{2}$$

$$+ \zeta\zeta'(k\zeta' - k'\zeta)/\Big(W_{1}W_{2}^{2}\Big)$$

$$- \zeta\zeta'(1/W_{2} - 2/W_{1})(2k\zeta'/W_{1} + k'\zeta/W_{2})/(2W_{2})$$

$$- g_{s}\zeta\zeta'^{2}[1/W_{1}^{2} - 1/(W_{1}W_{2}) + 1/W_{2}^{2}]/(2W_{2}),$$

$$A_{\parallel} = P[-\kappa - 4N/7 + (g_{\parallel} - g_{s}) + 3(g_{\perp} - g_{s})/7],$$

$$A_{\perp} = P[-\kappa + 2N/7 + 11(g_{\perp} - g_{s})/14].$$

$$(1)$$

Here g_s (\approx 2.0023) is the spin-only value. *N* is the average covalence factor, characteristic of the covalence effect of the studied systems. ζ and ζ' are the spin-orbit coupling parameters, and k and k' are the orbital reduction coefficients, respectively. P and κ are, respectively, the dipolar hyperfine coupling parameter for the free central ion and the core polarisation constant. These quantities could be obtained by applying the normalisation conditions and the approximate relationships relevant to covalence factor *N* from the cluster approach [34-37].

The corresponding denominators W_1 and W_2 are the energy differences between the ground ${}^{2}B_{1g}$ and the excited ${}^{2}B_{2g}$ and ${}^{2}E_{g}$ states [38], respectively. Based on the energy matrices for a 3d9 ion in tetragonally elongated octahedra, these denominators are expressed in terms of the cubic crystal field (CF) parameter Dq and the tetragonal CF parameters *Ds* and *Dt*:

$$W_1 \approx 10 \ Dq$$
, $W_2 \approx 10 \ Dq - 3 \ Ds + 5 \ Dt$. (2)

In $Zn(en)_3(NO_3)_2$, the host cation–anion distance R_0 is about 2.193 Å [39]. In consideration of the slight size mismatching substitution, the reference impurity-ligand bonding length R can be determined from the empirical relationship $R \approx R_0 + (r_i - r_h)/2$, where $r_i \approx 0.87 \text{ Å } [40]$

and r_h (≈ 0.88 Å [40]) are the ionic radii for the impurity Cu^{2+} and host Zn^{2+} , respectively. This yields $R \approx 2.188 \text{ Å}$ for both copper centres. In view of the Jahn-Teller elongation distortions of the copper centres, the local Cu^{2+} N³⁻ bonding lengths parallel and perpendicular to the C₄ axis can be expressed in terms of the relative tetragonal elongation ΔZ and the reference bonding length R (Fig. 1a):

$$R_{\parallel} \approx R + 2 \Delta Z$$
, $R_{\perp} \approx R - \Delta Z$. (3)

Utilising the local geometrical relationship in Figure 1a, the tetragonal CF parameters can be determined for both copper centres from the superposition model [41]:

$$Ds \approx (4/7)\bar{A}_{2}(R) \left[(R/R_{\perp})^{t2} - (R/R_{\parallel})^{t2} \right],$$

$$Dt \approx (16/21)\bar{A}_{4}(R) \left[(R/R_{\perp})^{t4} - (R/R_{\parallel})^{t4} \right]. \tag{4}$$

Here $\bar{A}_2(R)$ and $\bar{A}_4(R)$ are the intrinsic parameters. For octahedral 3dⁿ clusters, the formulae $\bar{A}_4(R) \approx (3/4) Dq$ and $\bar{A}_2(R) \approx 9\bar{A}_4(R)$ [42–44] are valid in many systems and could be utilised here. The power-law exponents are taken as $t_2 \approx 3$ and $t_4 \approx 5$, respectively [45].

From the reference bonding length R and the Slatertype self-consistent field wave functions [46], the group overlap integrals S_{dpt} , S_{dpe} , S_{s} , and A are computed and listed in Table 1. Normally, covalence (or electron cloud admixtures) for the same $Cu^{2+}-N^{3-}$ bonds may be slightly weaker at RT than low temperature (4.2 K); the cubic CF parameters Dq and the covalence factors N can be obtained for the studied systems from the optical spectral analysis for Cu²⁺ in nitrides [23] and collected in Table 1. The normalisation coefficients and the orbital admixture factors can be computed from the cluster approach [34-37]. Applying the free-ion values ζ_d^0 (\approx 829 cm⁻¹ [47]) for Cu^{2+} and ζ_p^0 (\approx 75 cm⁻¹ [48]) for N³⁻, the spin-orbit coupling parameters and the orbital reduction coefficients are obtained from the cluster approach [34-37]. As regards hyperfine structure constants, the dipolar hyperfine coupling parameter P is 402×10^{-4} cm⁻¹ [49]. The core polarisation constants k are estimated from the expectation values (≈ 0.3 [47]) for 3dⁿ ions in crystals and listed in Table 1, as the weaker covalence at RT may be associated with higher magnitude (average) of hyperfine structure constants and hence with the larger k. Thus, there is only one unknown quantity (i.e. the relative tetragonal elongation ΔZ) in the formulae of the SHPs. Substituting the related quantities into (1) and matching the calculated SHPs for the copper clusters to the measured results, one can obtain the optimal relative tetragonal elongations

$$\Delta Z \approx 0.005$$
 and 0.007 (5)

Table 1: Group overlap integrals, cubic field parameters (in cm⁻¹), covalence factors, normalisation coefficients, orbital admixture factors, spin-orbit coupling parameters (in cm⁻¹), and orbital reduction coefficients for the Cu(en)₃²⁺ clusters in Zn(en)₃(NO₃)₂ polycrystalline powder and the Ru(en)₃³⁺ cluster in the uniaxial [Rh(en)₃Cl₃]₂NaCl·6H₂O single crystal doped with the single-crystal chloride salt [Ru(en)₃]Cl₃·4H₂O at various temperatures (in K).

Cluster	Centre	т	$S_{ m dpt}$	S_{dpe}	S _{ds}	A	Dq	N	N t	N _e
Cu(en) ₃ ²⁺		4.2	0.0081	0.0256	0.0207	1.2172	1510	0.81	0.813	0.824
	II	RT	0.0081	0.0256	0.0207	1.2172	1510	0.84	0.842	0.852
$Ru(en)_3^{3+}$	l	4	0.0398	0.1012	0.0822	1.1518	2900	0.895	0.956	0.986
Cluster	Centre	T	λ_{t}	λ_{e}	λ_{s}	ζ	ζ′	k	k'	κ
Cu(en) ₃ ²⁺	ı	4.2	0.487	0.387	0.313	681	673	0.910	0.665	0.227
	II	RT	0.441	0.351	0.284	704	697	0.924	0.717	0.276
$Ru(en)_3^{3+}$	1	4	0.258	0.239	0.065	1130	1143	0.988	0.931	_

Table 2: g Factors and hyperfine structure constants (in 10^{-4} cm⁻¹) for the Cu(en)₃²⁺ clusters in Zn(en)₃(NO₃)₂ polycrystalline powder and the Ru(en)₃³⁺ cluster in the uniaxial [Rh(en)₃Cl₃]₂NaCl·6H₂O single crystal doped with the single-crystal chloride salt [Ru(en)₃]Cl₃·4H₂O.

Cluster	Centres	Т		g //	$oldsymbol{g}_{\perp}$	$oldsymbol{g}_{iso}$	A //	A_{\perp}	A
Cu(en) ₃ ²⁺	I	4.2	Calc.a	2.248	2.063	2.125	-168	21	-42
			Expt. ^b	2.248	2.082	_	-168	-	-
	II	RT	Calc. ^a	2.277	2.070	2.139	-182	7	-56
			Expt.b	-	_	2.139	_	-	-56
Ru(en) ₃ ³⁺	1	4	Calc. ^a	2.623	0.330	_	_	-	-
			Expt.b	2.640(22)	0.330(7)	_	-	-	-

^aThis work. ^bStanko et al. [17] and Bertini et al. [18].

for centres I and II, respectively. The corresponding SHPs are given in Table 2.

2.3 Calculations for the $Ru(en)_3^{3+}$ Cluster

The Ru(en)₃³⁺ cluster in the diamagnetic and uniaxial [Rh(en)₃Cl₃]₂NaCl·6H₂O single crystal doped with [Ru(en)₃]Cl₃·4H₂O may conserve the original trigonal (D_{3d}) symmetry of the host Ru³⁺ site with the metal–ligand bonding lengths R_1 (≈2.102 Å) and R_2 (≈2.117 Å) [32]. For a trigonally distorted octahedral 4d⁵ (Ru³⁺) cluster, the perturbation formulae of the anisotropic g factors can be expressed as [22, 30, 31]:

$$g_{//} = 2|(1+k)\cos^2 \alpha - \sin^2 \alpha|,$$

 $g_{\perp} = 2|k'\sin 2\alpha/\sqrt{2} + \sin^2 \alpha|,$ (6)

with

$$\alpha = \frac{\pi}{2} + \frac{1}{2} \arctan \frac{\sqrt{2}\zeta'}{\frac{\zeta}{2} - V}.$$
 (7)

Here V is the trigonal CF parameter. The Ru(en)₃³⁺ cluster in [Rh(en)₃Cl₃]₂NaCl·6H₂O single crystal may suffer some lattice modification related to the host [Ru(en)₃]Cl₃·4H₂O due to the excess sodium chloride. For

example, the effective $Ru^{3+}-N^{3-}$ bonding angle β related to the C_3 axis can be changed, characterised by an angular variation $\Delta\beta$ with respect to the host angle β_H (\approx 57.32° [17, 32]) (Fig. 1b). By using the local structure and the superposition model [35, 50–53], the trigonal CF parameter can be expressed as follows:

$$V = -[(9/7)\bar{A}_{2}(R)(R/R_{1})^{t2}(3\cos^{2}\beta - 1)$$

$$+ (20/21)\bar{A}_{4}(R)(R/R_{1})^{t4}(35\cos^{4}\beta - 30\cos^{2}\beta + 3)$$

$$+ (20\sqrt{2}/3)\bar{A}_{4}(R)(R/R_{1})^{t4}\sin^{3}\beta\cos\beta]$$

$$- [(9/7)\bar{A}_{2}(R)(R/R_{2})^{t2}(3\cos^{2}\beta - 1)$$

$$+ (20/21)\bar{A}_{4}(R)(R/R_{2})^{t4}(35\cos^{4}\beta - 30\cos^{2}\beta + 3)$$

$$+ (20\sqrt{2}/3)\bar{A}_{4}(R)(R/R_{2})^{t4}\sin^{3}\beta\cos\beta].$$
 (8)

Here the reference bonding length R is conveniently taken as the average of R_1 and R_2 . $t_2 \approx 3$ and $t_4 \approx 5$ [45] are the power-law exponents. $\bar{A}_2(R)$ and $\bar{A}_4(R)$ are the intrinsic parameters. For 4dⁿ ions under octahedral CFs, the relationships $\bar{A}_4(R) \approx (3/4) D_q$ and $\bar{A}_2(R) \approx 9\bar{A}_4(R)$ [42–44] could be utilised here.

From the reference distance R and the Slater-type self-consistent field wave functions [46], the group overlap integrals $S_{\rm dpt}$, $S_{\rm dpe}$, $S_{\rm s}$, and A are computed and listed in Table 1. The spectral parameters $D_{\rm q}$ and N are obtained from the optical spectral analysis for Ru³⁺ in nitrides [23]

and also listed in Table 1. The related normalisation coefficients N_v and the orbital admixture factors λ_v (or λ_s) can be calculated from the cluster approach [34–37]. Utilising the free-ion values ζ_d^0 (Ru³⁺) \approx 1180 cm⁻¹ [22] and ζ_p^0 $(N^{3-}) \approx 75 \text{ cm}^{-1}$ [49], the spin-orbit coupling parameters and the orbital reduction coefficients are calculated from the cluster approach [34–37] and given in Table 1. Substituting these quantities into (6) and matching the calculated g factors to the measured results [17], one can obtain the optimal local angular variation

$$\beta \approx 55.47^{\circ}$$
 or $\Delta\beta \approx -1.85^{\circ}$. (9)

The corresponding *g* factors are given in Table 2.

Discussion

Table 2 reveals that the calculated SHPs for all the $Cu(en)_3^{2+}$ and $Ru(en)_3^{3+}$ clusters based on the local lattice distortions (i.e. the relative tetragonal elongations ΔZ and the local angular variation $\Delta\beta$) agree well with the measured results at various temperatures. Thus, the EPR spectra and local structures for these Cu(en)₃²⁺ and Ru(en)₃³⁺ clusters are systematically in a uniform manner.

(A) In general, the microscopic mechanisms of the local structural modifications for the Cu(en)₃²⁺ and Ru(en)₃³⁺ clusters related to the host lattices may be explained as the Jahn-Teller effect and size mismatch. For the Cu(en)₃²⁺ clusters (centres I and II), the positive relative tetragonal elongations ΔZ in (5) are in accordance with the expectation based on the positive anisotropies $\Delta g \, (= g_{\parallel} - g_{\perp})$ of the experimental g factors [17]. Despite the original trigonal point symmetry of host Zn²⁺ site in $Zn(en)_3(NO_3)_2$ single crystal, the impurity Cu^{2+} ion tends to exhibit tetragonal elongation distortion because of the Jahn-Teller effect through the vibration interactions, which can completely remove the two-fold orbital degeneracy of the cubic ground state ${}^{2}E_{\rm g}$. Comparatively, the influence of the size mismatch can be much weaker than the Jahn-Teller effect due to the very small difference in ionic radius between Cu^{2+} and Zn^{2+} . Nevertheless, the tetragonal elongations ΔZ of both copper centres I and II are much smaller than those (0.08 \sim 0.3 Å) [35, 54, 55] of other similar copper centres in some tetragonally elongated octahedra [e.g. AgCl, NaCl, alkali lead tetraborate $90R_2B_4O_7 \cdot 9PbO \cdot CuO$ (R = Li, Na, and K) glasses and LaSrGa_{0.995}Cu_{0.005}O₄ ceramics] of the same Jahn–Teller nature. This point may be illustrated as the stronger CFs and hence larger force constant of the copper-ligand bonds

in present Cu(en)₃²⁺ clusters, based on the spectrochemical series [23]. Moreover, the slightly larger axial elongation ΔZ of copper centre II than centre I can be suitably attributed to be more intense vibration interactions at RT. On the other hand, the significant angular variation (decrease) by about 2° for the Ru(en)₃³⁺ cluster is mainly attributable to the Jahn-Teller effect. Notably, the local angular variation $\Delta\beta$ for present Ru(en)₃³⁺ cluster in uniaxial [Rh(en)₃Cl₃]₂NaCl·6H₂O single crystal doped with [Ru(en)₃]Cl₃·4H₂O is slightly smaller in magnitude than those for the similar trigonal (D_{3d}) Ru³⁺ centres in the garnets [26]. This is understandable in view of the local angular variations arising from both the Jahn-Teller effect and the significant size mismatch between the impurity Ru^{3+} ($\simeq 0.87 \text{ Å } [40]$) and host Al^{3+} ($\simeq 0.54 \text{ Å } [40]$) or Ga^{3+} (~0.62 Å [40])

(B) The characteristic of the SHPs for these clusters can be further illustrated as follows. First, the observed positive g anisotropy Δg for copper centre I arises from the lowest ${}^{2}B_{1g}$ state due to the tetragonal elongation. The average g_{iso} of g factors (and also the average |A| for hyperfine structure constants) for copper centre II is slightly higher than centre I, owing to the slightly weaker covalence at RT in the former. Of course, the presently calculated g factors for centre II remain to be further checked with experimental measurements. Second, although the sign of the average of hyperfine structure constants was not determined experimentally in [18] at RT, the results $A_{\parallel} < 0$ and $A_{\perp} > 0$ in current calculations are consistent with various experimental values and theoretical expectations [35, 49, 56] for tetragonally elongated octahedral Cu^{2+} centres. The negative A_{\parallel} is due to the positive anisotropic terms for hyperfine structure constants smaller than the magnitudes of the negative isotropic terms related to k, arising from the Fermi contact interactions due to the Cu²⁺ 3d-3s (or -4s) configuration interactions. And, the positive A_{\perp} is attributable to the negative isotropic terms slightly lower in magnitude than the positive anisotropic ones (1). Meanwhile, the slightly larger magnitude of hyperfine structure constants of centre II than centre I could be ascribed to the higher N and κ of the former. Third, the positive anisotropy Δg for the Ru(en)₃³⁺ cluster is due to the trigonal elongation distortion, which is much larger than the Ru^{3+} site in host $[Ru(en)_3]Cl_3 \cdot 4H_2O$. This indicates that the Jahn-Teller effect may tend to yield trigonal elongation distortion of the ligand octahedron for a Ru³⁺ cluster. This is somewhat similar to the Ru³⁺ centres in the garnets except much stronger influence arising from the size mismatch in the latter [26].

(C) The much larger anisotropy Δg of the Ru(en)₃³⁺ cluster than the Cu(en)₃²⁺ clusters can be further

illustrated here. First, the orbital angular momentum shows larger contribution to Δg for the cubic ground triplet $^{2}T_{2g}$ of the Ru(en) $_{3}^{3+}$ cluster than that for the cubic ground doublet ${}^{2}E_{g}$ of the Cu(en) $_{3}^{2+}$ cluster. Of course, both systems exhibit significant anisotropic contributions to g factors due to the axial symmetrical distortion and spinorbit coupling interactions, as compared with the cases of cubic orbital singlets (e.g. ${}^4A_{2g}$ and ${}^3A_{2g}$ ground states for octahedral 3d³ and 3d⁸ clusters [22, 23]). Second, different axial symmetries (i.e. trigonality and tetragonality) for the $Ru(en)_3^{3+}$ and $Cu(en)_3^{2+}$ clusters may involve dissimilar mechanisms of the contributions to Δg . In detail, the ganisotropy arises from the first-order and second-order perturbation terms for the Ru(en)₃³⁺ and Cu(en)₃²⁺ clusters ((6) and (1)), respectively, which leads to the much larger Δg in the former. Finally, the more significant axial distortion $\Delta\beta$ for the Ru(en)₃³⁺ cluster than the much smaller ΔZ for the Cu(en)₃²⁺ clusters may also induce much larger Δg in the former.

4 Conclusion

The SHPs and the local structures for the tetragonally elongated Cu(en)₃²⁺ clusters and the trigonally elongated Ru(en)₃³⁺ cluster at various temperatures are theoretically studied by using the perturbation computations. The Cu²⁺ centres I and II are found to experience the slight relative tetragonal elongations ΔZ of about 0.005 and 0.007 Å along the C₄ axis due to the Jahn-Teller effect at 4.2 K and RT, respectively. In the Ru(en)₃³⁺ clusters, the impurityligand bonding angle β suffers the significant decrease $\Delta\beta$ by about 1.85° related to the host [Ru(en)₃]Cl₃·4H₂O owing to the Jahn-Teller effect at 4 K. The calculated g factors and hyperfine structure constants based on the above local structural parameters (the relative tetragonal elongation ΔZ and the angular distortion $\Delta \beta$) agree well with the measured values. Present theoretical studies would be helpful to understand the local structural properties and may establish an improved scheme for the systematic apprehending of the unique behaviours for various Jahn-Teller impurities (e.g. 3d⁹ and 4d⁵ ions) in ethylenediamine and the relevant complexes (or other similar crystals [57-59]).

Acknowledgements: This work was financially supported by the National Natural Science Foundation of China (Grant No. 11764028).

Conflicts of interest: There are no conflicts to declare.

References

- [1] L. Qin, X. Li, J. Q. Zhu, W. C. Li, H. Xu, et al., Ind. Crop. Prod. 102, 51 (2017).
- [2] J. P. Stanford, P. H. Pfromm, and M. E. Rezac, J. Appl. Polym. Sci. 134, 44771 (2017).
- [3] D. K. Das, J. Kumar, A. Bhowmick, P. Kr. Bhattacharyya, and S. Banu, Inorg. Chim. Acta. 462, 167 (2017).
- [4] Z. Li, Y. Zhang, Q. Niu, M. Mou, Y. Wu, et al., J Lumin. 187, 274
- [5] L. Bai, H. Liu, F. Qiao, and H. Yan, Food Chem. 230, 154 (2017).
- [6] Y. Li, C. C. Huang, J. B. Zheng, and H. L. Qi, Biosens. Bioelectron. 38, 407 (2012).
- [7] K. Mech, J. Mech, P. Zabinski, R. Kowalik, and M. Wojnicki, J. Elecroanal. Chem. 748, 76 (2015).
- M. Yagi, M. Kasamastu, and M. Kaneko, J. Mol. Catal. A-Chem. **151**, 29 (2000).
- A. L. Crumbliss, S. C. Perine, A. Kirk Edwards, and D. P. Rillema, J. Phys. Chem. 96, 1388 (1992).
- [10] V. Moses, Ö. T. Bishop, and K. A. Lobb, Chem. Phys. Lett. 678, 91 (2017).
- [11] S. Pramodini Devi, N. Shantibala Devi, L. Jaideva Singh, R. K. Bindiya Devi. W. Radhapiyari Devi. et al., Inorg. Nano-Met. Chem. 47, 223 (2017).
- [12] S. Dhar, M. Nethaji, and A. R. Chakravaty, Inorg. Chem. Acta. 358, 2437 (2005).
- [13] I. Qasim, M. W. U. Rehman, M. Mumtaz, G. Hussain, K. Nadeem, et al., J. Alloy. Compd. 649, 320 (2015).
- [14] H. M. Zhang, S. Y. Wu, P. Xu, L. L. Li, and S. X. Zhang, Eur. Phys. J. Appl. Phys. 50, 30901 (2010).
- [15] X. S. Liu, S. Y. Wu, S. Y. Zhong, L. J. Zhang, and F. Zhang, Russ. J. Phys. Chem. A+ 92, 2744 (2018).
- [16] H. M. Zhang, S. Y. Wu, and M. Q. Kuang, Comput. Theor. Chem. 984, 137 (2012).
- [17] J. A. Stanko, H. J. Peresie, R. A. Bernheim, R. Wang, and P. S. Wang, Inorg. Chem. 12, 634 (1973).
- [18] I. Bertini, D. Gatteschi, and A. Scozzafava. Inorg. Chem. 16, 1973 (1977).
- [19] P. V. Bernhardt and M. J. Riley, Aust. J. Chem. 56, 287 (2003).
- [20] R. D. Peacock and B. Stewart, Chem. Commun. 5, 295 (1982).
- [21] N. Norani, H. Rahemi, S. F. Tayyari, and M. J. Riley, J. Mol. Model. 15, 25 (2009).
- [22] A. Abragam and B. Bleaney, Electron Paramagnetic Resonance of Transition Ions, Oxford University Press, London 1970.
- [23] A. S. Chakravarty, Introduction to the Magnetic Properties of solids, Wiley-Interscience Publication, New York 1980.
- [24] Y. V. Yablokov and T. A. Ivanova, Coord. Chem. Rev. 1255, 190 (1999).
- [25] C. Koepke, K. Wisniewski, and M. Grinberg, J. Alloy. Compd. **341**, 19 (2002).
- [26] S. Y. Wu, Q. Fu, J. Z. Lin, and H. M. Zhang, Opt. Mater. 29, 1014 (2007).
- [27] Q. Fu, S. Y. Wu, J. Z. Lin, and J. S. Yao, Pramana-J. Phys. 68, 499
- [28] S. Y. Wu, Q. Fu, H. M. Zhang, and G. D. Lu, J. Alloy. Compd. 455, 42 (2008).
- [29] S. Y. Wu, Q. Fu, J. S. Yao, and H. M. Zhang, Radiat. Eff. Defect. S. 162, 627 (2007).

- [30] S. Geschwind and J. P. Remeika, J. Appl. Phys. 33, 370
- [31] T. J. O'Reilly and E. L. Offenbacher, J. Chem. Phys. 54, 3065 (1971).
- [32] H. J. Peresie and J. A. Stanko, J. Chem. Soc. D 1674 (1970).
- [33] W. H. Wei, S. Y. Wu, and H. N. Dong, Z. Naturforsch. A 60, 541 (2005).
- [34] Y. X. Hu, S. Y. Wu, and X. F. Wang, Philosoph. Mag. 90, 1391 (2010).
- [35] M. Q. Kuang, S. Y. Wu, G. L. Li, and X. F. Hu, Mol. Phys. 113, 698
- [36] C. C. Ding, S. Y. Wu, G. L. Li, and Y. Q. Xu, Phys. B 459, 129 (2015).
- [37] M. Q. Kuang, S. Y. Wu, B. T. Song, L. L. Li, and Z. H. Zhang, Optik 124, 892 (2013).
- [38] C. Koepke, K. Wisniewski, and M. Grinberg, J. Alloy. Compd. 341, 19 (2002).
- [39] D. Neill, M. J. Riley, and C. H. L. Kennard, Acta Cryst. C53, 701 (1997).
- [40] R. D. Shannon, Acta Crystallogr. A 32, 751 (1976).
- [41] D. J. Newman and B. Ng, Rep. Progr. Phys. 52, 699 (1989).
- [42] H. M. Zhang, S. Y. Wu, Y. X. Hu, and X. F. Wang, J. Supercond. Nov. Magn. 23, 833 (2010).
- [43] X. F. Hu, S. Y. Wu, M. Q. Kuang, and G. L. Li, Z. Naturforsch. A 69, 562 (2014).
- [44] Y. X. Hu, S. Y. Wu, X. F. Wang, and P. Xu, Eur. Phys. J. D 58, 281 (2010).

- [45] H. M. Zhang, S. Y. Wu, P. Xu, and L. L. Li, J. Mol. Struct.-Theochem. 953, 157 (2010).
- [46] E. Clementi, D. L. Raimondi, and W. P. Reinhardt, J. Chem. Phys. 47, 1300 (2010).
- [47] J. S. Griffith, The Theory of Transition-Metal Ions, Cambridge University Press, London 1964.
- [48] D. W. Smith, J. Chem. Soc. A 92, 3108 (1970).
- [49] B. R. McGarvey, J. Phys. Chem. 71, 51 (1967).
- [50] H. M. Zhang, S. Y. Wu, M. Q. Kuang, and Z. H. Zhang, J. Phys. Chem. Solids 73, 846 (2012).
- [51] S. Y. Wu, H. M. Zhang, P. Xu, and S. X. Zhang, Spectrochim. Acta A 75, 230 (2010).
- [52] L. L. Li, S. Y. Wu, P. Xu, and S. X. Zhang, Phys. Chem. Miner. 37, 497 (2010).
- [53] H. M. Zhang, S. Y. Wu, P. Xu, and L. L. Li, Mod. Phys. Lett. B 24, 2357 (2010).
- [54] Y. K. Cheng, S. Y. Wu, C. C. Ding, and M. Q. Kuang, J. Appl. Spectr. 81, 1064 (2015).
- [55] C. C. Ding, S. Y. Wu, Y. K. Cheng, and L. J. Zhang, Int. J. Mod. Phys. B 29, 1542015 (2015).
- [56] J. L. Rao, G. Sivaramaiah, and N. O. Gopal, Phys. B 349, 206 (2004).
- [57] D. Li, X. Zu, D. Ao, Q. Tang, Y. Fu, et al., Sensor. Actuat. B-Chem. 294, 55 (2019).
- [58] D. Li, Y. Tang, D. Ao, X. Xiang, S. Wang, et al., Int. J. Hydrogen Energ. 44, 3985 (2019).
- [59] C. Cai, S. Han, W. Liu, K. Sun, L. Qiao, et al., Appl. Catal. B-Environ. 260, 118103 (2020).